sustainability

MDPI

Article

Air Pollution and Dispersion of Airborne Chemical Elements in Klaipėda Seaport-City

Aistė Andriulė [1,*], Sergej Suzdalev [1], Erika Vasiliauskienė [1,2] and Inga Dailidienė [1,3]

[1] Marine Research Institute, Klaipeda University, H. Manto Str. 84, 92294 Klaipeda, Lithuania; sergej.suzdalev@ku.lt (S.S.); erika.vasiliauskiene@ku.lt (E.V.); inga.dailidiene@ku.lt (I.D.)
[2] Department of Business Administration, Klaipeda State University of Applied Sciences, 91223 Klaipeda, Lithuania
[3] Science of Technology, Lithuanian Business College, 91249 Klaipeda, Lithuania
* Correspondence: aiste.andriule@ku.lt; Tel.: +370-64145744

Abstract: This study examines the spatial distribution of chemical elements in the urban environment of Klaipėda Seaport City, assessing their concentrations in industrial, residential, and port zones. Particulate matter (PM) samples were collected using passive sampling methods and analyzed for their chemical composition to identify pollution patterns. Beyond spatial pollution analysis, a detailed correlation analysis of pollutants was conducted to determine potential emission sources across different functional city zones. The results indicate significantly elevated concentrations of heavy metals in port and transport zones, highlighting the necessity for targeted air quality improvement measures and innovative pollution mitigation strategies.

Keywords: Klaipėda city; air pollution; chemical elements; particulate matter; nitrogen dioxide; spatial analysis; pollution correlation; sustainability; urban planning; environmental protection

Academic Editor: Pallav Purohit

Received: 16 March 2025
Revised: 5 April 2025
Accepted: 7 April 2025
Published: 24 April 2025

Citation: Andriulė, A.; Suzdalev, S.; Vasiliauskienė, E.; Dailidienė, I. Air Pollution and Dispersion of Airborne Chemical Elements in Klaipėda Seaport-City. *Sustainability* **2025**, *17*, 3834. https://doi.org/10.3390/su17093834

1. Introduction

Air pollution is one of the most significant environmental challenges of the 21st century, posing serious threats to ecosystems and public health worldwide. Pollutants such as nitrogen dioxide (NO_2), particulate matter (PM_{10}, $PM_{2.5}$), and other airborne compounds are well-studied for their negative impact on respiratory, cardiovascular, and neurological health. While urban air pollution studies often focus on pollutant concentrations, the chemical composition of particulate matter and its spatial distribution receive less attention, especially in port cities where various pollution sources intersect.

Klaipėda, Lithuania's main seaport and industrial hub, is a unique case for studying the interaction of urban, industrial, and maritime pollution. Unlike many European ports located in peripheral areas, Klaipėda's port activities are closely integrated into the city's urban environment. As a result, city residents directly experience the impact of port operations on air quality. The close proximity of port terminals, cargo handling, industrial sites, and residential areas creates a complex pollution distribution structure.

One of the primary sources of air pollution in Klaipėda is maritime transport. The combustion of low-quality marine fuels releases sulfur oxides, nitrogen oxides, and fine particulate matter into the atmosphere [1]. Additionally, pollution is exacerbated by heavy-duty freight transport within the port and on city roads. Trucks emit NO_2, particulate matter, and trace metals such as zinc, copper, and nickel [2]. The convergence of these pollution

sources within the city contributes to a complex pollution dynamic, necessitating detailed investigations to identify the key contributors and develop effective mitigation strategies.

Klaipėda's coastal location also presents challenges for air quality management. While coastal regions often experience strong winds that help disperse pollutants, urban infrastructure can hinder air mass movement. Dense construction, tall buildings, and industrial zones act as physical barriers, reducing wind speed and allowing pollutants to accumulate in specific areas [3]. As a result, pollution distribution in the city is not uniform: port areas and industrial zones tend to have higher metal concentrations, whereas residential districts are more affected by emissions from local transport and heating systems.

Despite extensive studies on pollutant concentrations in urban areas, relatively little attention has been given to the chemical composition of particulate matter in port cities—especially those where industrial and residential zones coexist in close proximity. Many air quality studies, including a previous investigation conducted in Klaipėda on which the current research is based [4], have focused primarily on total PM mass concentrations without analyzing the elemental composition of airborne particles. While such measurements are valuable for assessing general pollution levels, they do not provide insight into the sources or toxicity of specific trace elements.

This study addresses that methodological gap by examining the chemical composition and spatial distribution of PM across Klaipėda, offering a deeper understanding of pollutant sources, transport mechanisms, and potential health impacts in a complex urban–port setting. Such knowledge is critical not only for scientific assessment but also for designing targeted, evidence-based air quality management strategies.

The aim of this study is to assess the chemical composition of airborne particulate matter in Klaipėda, with the goal of identifying major pollution sources and evaluating the role of meteorological conditions in pollutant dispersion. Effective air pollution management requires both meteorological analysis and sustainable urban planning solutions. Better urban planning can enhance air circulation and reduce pollutant accumulation in specific areas. This study, therefore, analyzes the chemical composition of particulate matter and the meteorological potential for pollutant dispersion to better understand air quality variations in the city and propose effective pollution reduction strategies.

2. Materials and Methods

2.1. Study Area

Klaipėda (54°43′16″ N, 21°07′ E) is located on the southeastern coast of the Baltic Sea and is Lithuania's third-largest city, as well as its most significant seaport (Figure 1). The city covers approximately 98 km^2 and has a population of around 166,000 inhabitants. It belongs to the southeastern Baltic region, which is characterized by a temperate maritime climate and lowland terrain composed mainly of sandy and clayey soils formed during glacial and post-glacial periods. The proximity of the Curonian Lagoon and the Baltic Sea strongly influences Klaipėda's local climate, particularly in terms of temperature moderation, humidity levels, and prevailing wind patterns.

The urban layout of Klaipėda is predominantly linear, extending approximately 16 km in a north-south direction. This spatial configuration has been shaped by the historical development of the city as a port and logistics hub. The Port of Klaipėda, one of the most important maritime gateways in the region, handles more than 7000 vessels annually from over 70 countries and is situated adjacent to the city center. Due to this close integration, industrial, residential, and commercial areas are closely interwoven, forming a complex urban structure where economic activities and urban functions overlap.

The city's transportation network is structured around three major arterial corridors that support freight and passenger mobility. The primary corridor, running parallel to the

port, serves as the main industrial and logistics axis, facilitating the movement of goods and services. Two additional transport corridors connect the port to residential districts and inland regions, ensuring accessibility and regional connectivity. Additionally, railway lines run along the eastern and western edges of the city, playing a key role in freight transport and linking Klaipėda to national and international trade routes.

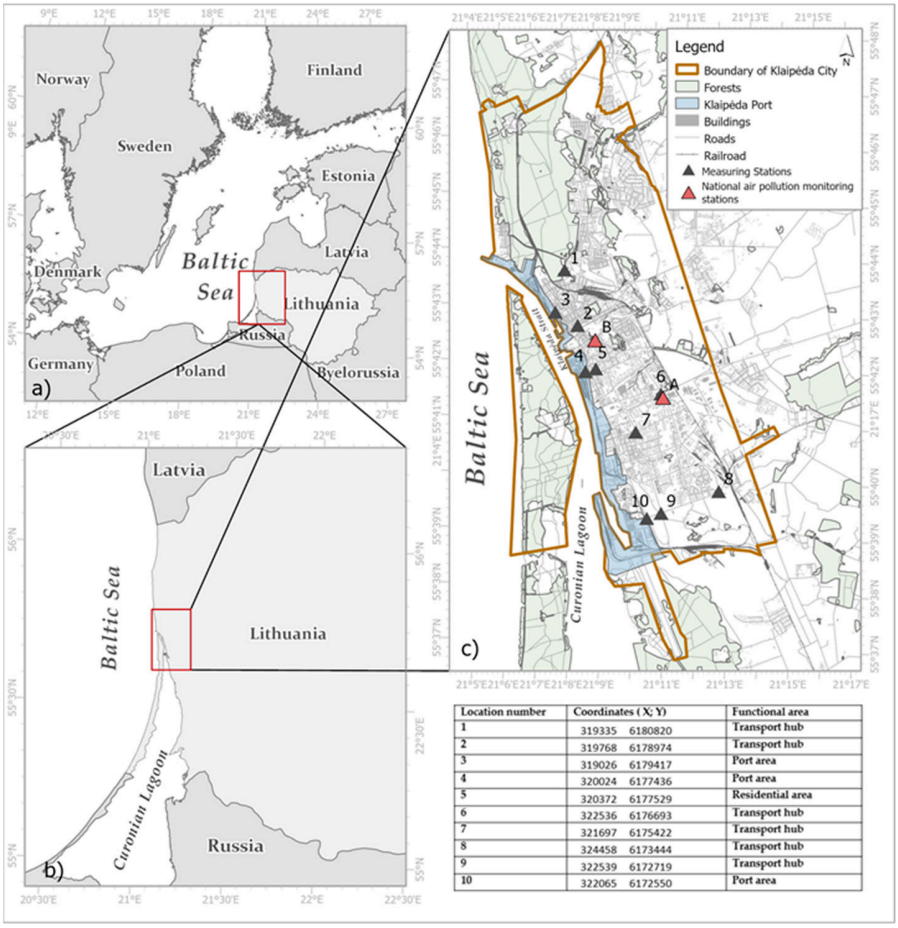

Location number	Coordinates (X; Y)	Functional area
1	319335 6180820	Transport hub
2	319768 6178974	Transport hub
3	319026 6179417	Port area
4	320024 6177436	Port area
5	320372 6177529	Residential area
6	322536 6176693	Transport hub
7	321697 6175422	Transport hub
8	324458 6173444	Transport hub
9	322539 6172719	Transport hub
10	322065 6172550	Port area

Figure 1. The study area: southeast part (SE) of the Baltic Sea (**a**); Klaipeda Seaport-City (**b**); air pollution measuring stations (MS) by urban functional area (**c**).

Urban development in Klaipėda is currently shaped by two dominant trends: horizontal expansion in the northern part of the city and densification in the central districts. The northern expansion is characterized by the conversion of previously forested areas into residential zones, resulting in increased built-up areas and higher traffic volumes. In contrast, the city center is experiencing vertical densification, with the construction of office buildings, commercial complexes, and high-rise residential developments. These transformations reflect broader urbanization processes that influence land use distribution and spatial planning in Klaipėda.

The spatial proximity of residential, industrial, and transport infrastructure, combined with Klaipėda's dense maritime activity, creates a highly complex air pollution environment where multiple emission sources overlap. The interaction between port-related emissions, heavy-duty transport, and urban traffic patterns contributes to localized pollution hotspots, posing significant challenges for air quality management and urban sustainability.

2.2. Data and Methods

This study focuses on the analysis of particulate matter (PM), with nitrogen dioxide (NO_2) assessed as a supplementary air quality indicator. The methodology includes the

chemical composition analysis of PM, NO_2 monitoring, and statistical analysis to identify pollution sources and evaluate their impact on air quality dynamics. A comprehensive overview of all methodological stages is provided in Table A1, which outlines the sequential workflow from sampling to statistical interpretation.

Particulate matter (PM) was collected using dust collectors over extended eight-week sampling periods, designed to ensure sufficient particulate mass for chemical analysis. Sampling was conducted during four distinct seasons: summer from 5 July to 30 August 2023, autumn from 8 October to 3 December 2023, winter from 6 January to 2 March 2024, and spring from 2 March to 27 April 2024.

To evaluate air quality across Klaipėda, 10 monitoring locations out of 19th were selected (Figure 1). Three selected stations (No. 3, 4, 10) were in the port area, representing zones heavily impacted by maritime and industrial emissions along the port area. Six stations (no. 1, 2, 6, 7, 8, 9) were installed along two main Klaipeda streets to monitor pollution from vehicular traffic, forming the transport hub category. One station (no. 5) was positioned in a residential area near the port to provide a baseline for comparison with higher-emission zones (Figure 1). These locations were selected based on a prior study conducted by Andriulė et al. (2024) [4], specifically focusing on the sites where the highest concentrations of PM were recorded, providing sufficient material for chemical analysis.

Previous research has demonstrated that particulate matter (PM) concentrations tend to peak during the spring season. Accordingly, in this study, the chemical composition analysis of PM was conducted using the most recent seasonal data available prior to sample preparation. At sampling sites No. 6, No. 3, and No. 4, the PM mass collected during spring was sufficient for chemical analysis. However, at the remaining measurement locations, the spring dataset alone did not yield an adequate PM mass. To ensure the reliability and representativeness of the elemental analysis, the three most recent seasonal datasets—autumn, winter, and spring—were incorporated into the analysis for those locations, allowing for a more comprehensive evaluation of PM composition.

It is important to note that the study does not distinguish between $PM_{2.5}$ and PM_{10} fractions. This limitation arose due to the sampling method, which was designed to accumulate a sufficient total PM mass for chemical analysis across multiple trace elements, rather than to segregate particle sizes. As a result, the findings reflect the combined chemical composition of inhalable particles. While this approach enables broad characterization of elemental content in airborne particulate matter, it restricts the ability to evaluate specific health impacts or source contributions associated with different particle size fractions. Future research using size-segregated samplers is encouraged to provide more targeted insight into particle-specific pollution dynamics.

To maintain analytical precision, all collected dust particles underwent a standardized preparation protocol before chemical analysis. The samples were first dried in an oven at 45 °C for 1 h, with Petri dish lids removed to facilitate moisture evaporation, followed by a 30-min cooling period in a desiccator to eliminate residual moisture. The dried particles were then homogenized using an agate mortar and pestle, ensuring uniform particle size and eliminating larger fragments that could introduce variability in subsequent analyses. A precisely weighed 0.500XX g portion of wax was used as a binding matrix, to which 0.050XX g of homogenized dust was gradually added. The notation "XX" represents variable decimal values, which differ depending on the specific measurement recorded during sample preparation to maintain the required precision. If the total dust mass did not reach 0.050XX g, the sample was deemed unsuitable for further analysis. The prepared wax-dust mixture was then gently blended in a standard mortar, avoiding excessive pressure that could alter the sample properties, and was subsequently transferred onto a labeled A5 paper sheet for further analytical procedures. The chemical composition of dust samples

was determined using X-ray fluorescence (XRF) spectroscopy, performed with a SPECTRO XEPOS HE analyzer (manufactured by SPECTRO Analytical Instruments GmbH Boschstr.10, 47533 Kleve, Germany). This non-destructive analytical technique enabled the simultaneous detection of multiple elements with high precision and reproducibility, making it particularly suitable for multi-element environmental samples. The use of XRF allowed for the quantitative analysis of 59 chemical elements across all sampling sites.

Each sampling site was analyzed four times for chemical composition, and for this study, the average values were calculated to minimize random measurement errors. Measurements reported as below detection limits (BDL), indicated by the "<" symbol (e.g., <0.2 and other element-specific thresholds), were treated as the maximum possible detection limit rather than excluded or substituted with lower estimates. This approach follows established methodologies [5] and ensures that non-detectable concentrations are conservatively estimated rather than underestimated.

To further explore elemental distribution patterns and potential pollution sources, Spearman correlation analysis was applied to assess inter-element relationships across 10 monitoring locations in Klaipėda. A total of 59 elements were analyzed at each site, allowing for a comprehensive assessment of interdependencies within different functional zones of the city. The Spearman correlation method was selected due to its ability to detect monotonic relationships without assuming normal data distribution, making it particularly suitable for environmental studies, where concentration values often deviate from normality and may include measurements below detection limits.

To assess pollutant interactions, the analysis examined whether an increase in the concentration of one element corresponded with increases in others. This approach enabled the identification of anthropogenic pollution sources, particularly those associated with industrial and vehicular emissions, by evaluating whether such elements exhibited strong correlations ($r_s \geq 0.70$), indicating a common source. Moderate correlations ($0.40 \leq r_s < 0.70$) suggested potential relationships influenced by multiple factors, while weak or negligible correlations ($r_s < 0.40$) indicated limited direct association. Additionally, interactions between anthropogenic and naturally occurring elements were examined to assess potential environmental transformation processes, such as chemical reactions, resuspension, or atmospheric deposition.

Beyond elemental correlations, it was essential to examine how meteorological factors influence air pollution levels and dispersion patterns in Klaipėda. For this purpose, air quality data from state air pollution monitoring stations collected during 2020–2023 were analyzed alongside meteorological parameters recorded by the Lithuanian Hydrometeorological Service (LHMT) over the same period. These state monitoring stations, marked as points A and B on the map (Figure 1), were selected due to their high temporal resolution, providing hourly air pollutant concentration data. This temporal precision enabled a detailed evaluation of how short-term meteorological fluctuations affect air pollution dynamics. Station A, located in the central part of the city, and Station B, positioned near measurement site No. 6—an area significantly influenced by transport-related emissions—offered representative data for urban and industrial pollution sources.

In contrast, chemical composition analysis was conducted using passive samplers deployed at ten locations across the city. These samplers provided integrated pollutant concentrations over an eight-week period, making them suitable for chemical characterization but unsuitable for correlation analysis with meteorological variables. The low temporal resolution of passive sampling prevented the assessment of short-term variations in air pollution levels, necessitating the use of hourly datasets from state air pollution monitoring stations as the primary data source for meteorological correlation analysis.

These national stations continuously monitored PM and NO_2 concentrations, allowing for a robust evaluation of how meteorological variables—such as wind speed, wind direction, temperature, humidity, and atmospheric pressure—influenced both particulate matter and nitrogen dioxide levels. By integrating meteorological data with air pollution measurements, this analysis provided a comprehensive understanding of the factors affecting pollutant dispersion, accumulation, and transformation in Klaipėda's urban and industrial environment.

3. Results

3.1. Spatial Distribution of Chemical Elements in Klaipėda's Airborne Particulate Matter

The analysis of chemical elements in particulate matter (PM) is essential for identifying potential pollution sources in urban environments. In many scientific studies, air quality is assessed based on the total PM mass; however, this approach does not provide insights into the origin of pollution. Various factors influence air quality in Klaipėda, including industrial activities, the centrally located port, intensive heavy-duty traffic on main urban roads, and the potential contribution of naturally occurring aerosols. The city's spatial layout along the coastline and the predominant westerly air mass transport may affect the distribution of pollution components across the urban area. Therefore, to objectively assess air quality, it is crucial not only to quantify pollutant concentrations but also to determine their origin through chemical analysis—distinguishing between anthropogenic and natural sources.

This study takes a comprehensive approach by analyzing the chemical composition of PM and assessing whether the concentration of chemical elements is directly related to PM mass. Unlike studies that focus solely on total PM mass, this analysis provides a more detailed understanding of urban air quality by incorporating elemental composition as a key factor. Figure 2 presents the relationship between total PM mass and total chemical element content, allowing an evaluation of whether an increase in PM mass corresponds to a proportional increase in elemental concentrations or if this relationship varies depending on specific environmental and emission conditions.

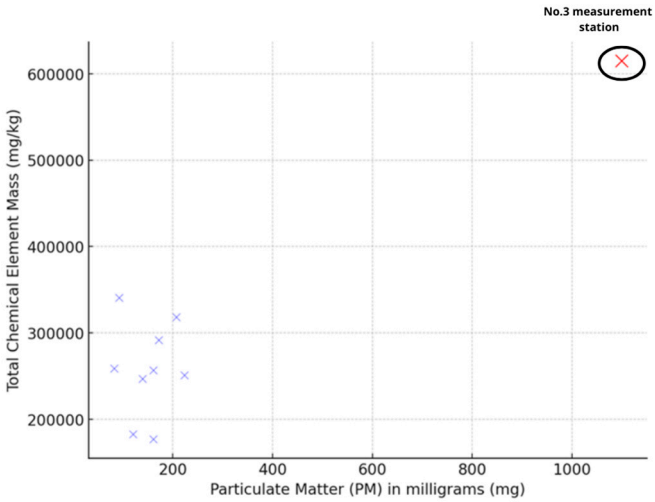

Figure 2. Relationship between total PM mass and chemical element concentration in airborne particulate matter in Klaipėda.

Figure 2 presents a scatter plot illustrating the relationship between PM mass and the total chemical element content in PM mass, based on measurements from ten sampling sites in Klaipėda. The vertical axis represents the total concentration of chemical elements (mg/kg), indicating the amount of chemical elements per kilogram of PM. The horizontal

axis shows the total PM mass (mg), determined by weighing the collected particulate matter on Petri dishes.

The diagram (Figure 2) clearly shows that there is no distinct linear relationship between total PM mass and the concentration of chemical elements—the data points are scattered, and no consistent trend is observed where an increase in PM mass would proportionally correspond to a higher concentration of chemical elements. Most measurement points are clustered within the lower PM mass range (below 300 mg), yet their chemical element concentrations are not constant, fluctuating between approximately 180,000 mg/kg and 350,000 mg/kg, regardless of PM mass. This indicates that the distribution of chemical elements within PM is not directly proportional to the total amount of particulate matter but is instead influenced by specific emission sources and the chemical composition of aerosols they generate.

A significant outlier is observed at the No. 3 station with PM mass reaching 1099.1 mg and chemical element concentrations exceeding 600,000 mg/kg—the highest values recorded among all sampled locations. This point is specifically highlighted in red to scientifically emphasize its exceptional nature within the dataset. It represents a functional area in Klaipėda city dominated by port activities, characterized by intense bulk cargo handling, maritime shipping, and vehicular traffic. Despite these significantly high pollution levels, subsequent analyses revealed that most detected chemical elements at this site are of natural origin, including sodium (Na), calcium (Ca), and silicon (Si). Sodium commonly occurs in fertilizers, calcium is typical in lime-based fertilizers and construction materials, and silicon is characteristic of sand and various mineral substances. The dominance of these elements strongly suggests emissions predominantly originate from bulk cargo handling, particularly fertilizers.

Despite the exceptional values observed at the No. 3 point, the overall analysis indicates no clear correlation between total PM mass and chemical element concentrations. High chemical element concentrations in samples with relatively low PM mass can be attributed to fine particulate matter ($PM_{2.5}$), which, due to its large surface area per unit mass, effectively adsorbs higher concentrations of heavy metals such as vanadium (V), nickel (Ni), lead (Pb), arsenic (As), and cadmium (Cd) from combustion and industrial emissions [6]. Conversely, coarser particles (PM_{10}), predominantly crustal in origin, tend to carry fewer pollutants [7]. Given that this study does not differentiate between $PM_{2.5}$ and PM_{10}, the precise contributions of fine and coarse particles to chemical element accumulation remain uncertain. Additional size-segregated analyses would be valuable in clarifying the distinct roles of fine and coarse particulate matter, further elucidating the impacts of maritime and industrial emissions on air quality. Processes such as secondary aerosol formation and selective particle deposition may also significantly influence the elemental composition of PM, highlighting why smaller PM masses sometimes exhibit higher chemical element concentrations. Therefore, evaluating not only total PM mass but also the chemical element composition is essential for comprehensively assessing urban air quality. For instance, despite the high PM mass at sampling station No. 3, the detected chemical elements were largely natural, posing comparatively lower health risks. In contrast, smaller PM mass samples with higher elemental concentrations may reflect anthropogenic pollution sources, such as vehicular emissions, potentially associated with greater environmental and human health hazards. Thus, analyzing chemical elements at each measurement site is vital to objectively assess air quality, accurately identify emission sources, and reveal risks that remain hidden when relying solely on PM mass-based threshold values.

To analyze the distribution of chemical elements across Klaipėda, we developed a series of maps (Figure 3) that visually represent the chemical composition of PM at all 10 sampling sites. Figure 3a illustrates the most dominant chemical elements at each

sampling location, providing insights into the spatial variability of pollutants within the city, while Figure 3f depicts the lowest detected concentrations of chemical elements, allowing for an assessment of background pollution levels in the urban environment. The maps in Figure 3a–f show a decreasing order of chemical element concentrations at each sampling site, offering a comprehensive visualization of pollutant intensity and distribution.

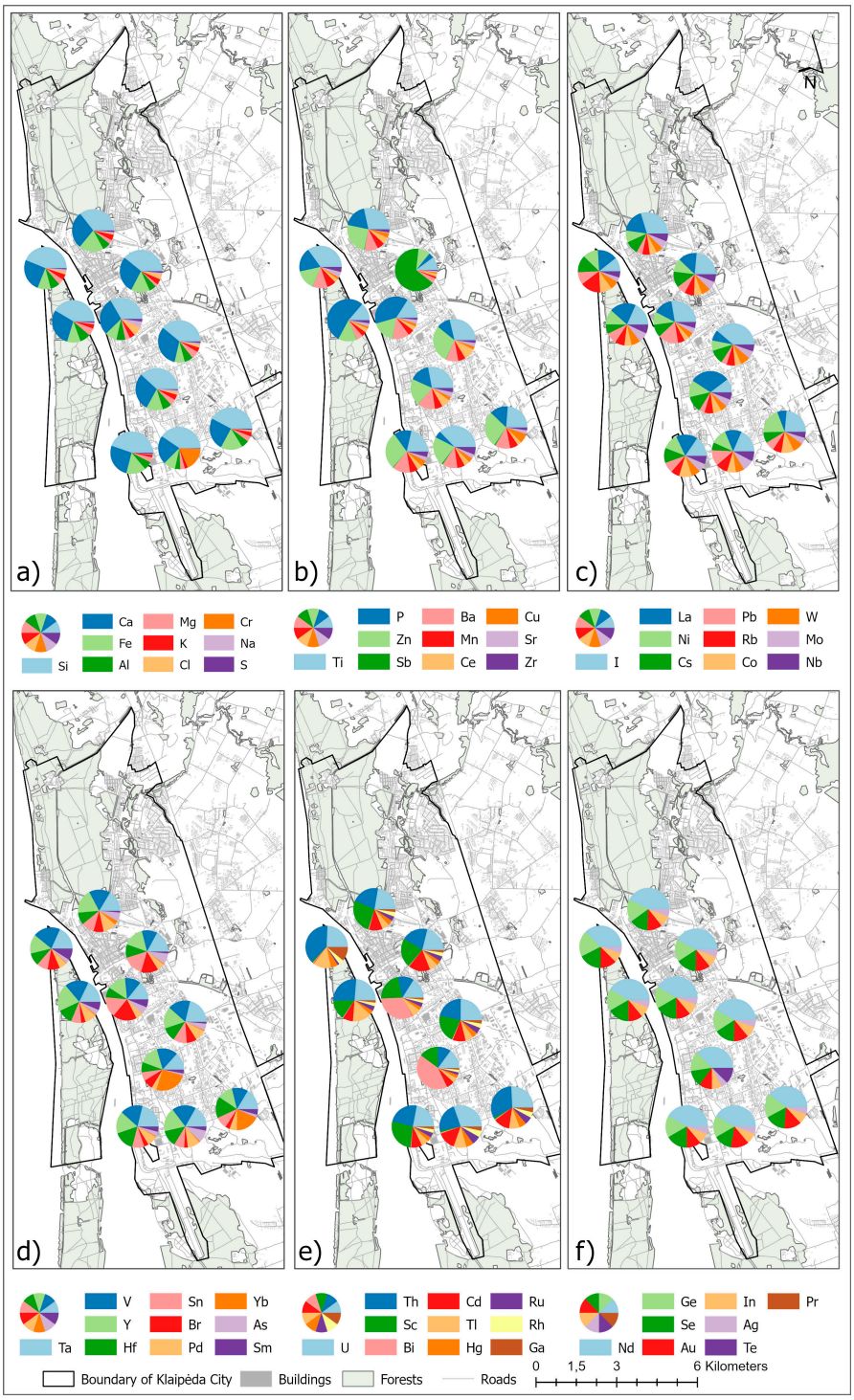

Figure 3. Chemical element composition of particulate matter (PM) across sampling locations in Klaipėda ((**a**–**f**): highest to lowest concentrations).

This spatial representation highlights the dominant pollutants across different areas of the city, serving as a foundation for further analysis using correlation methods to evaluate

potential emission sources. By integrating this spatial data with advanced statistical methods, this study provides a more in-depth assessment of pollutant behavior and its potential origins.

To assess the differences in chemical element concentrations across Klaipėda, the spatial distribution map (Figure 3) is supplemented with logarithmic chemical element dispersion scales (Figure 4). The integration of spatial distribution with concentration diagrams, which highlight element increases at specific measurement sites, allows for a comprehensive analysis of urban contamination by chemical elements.

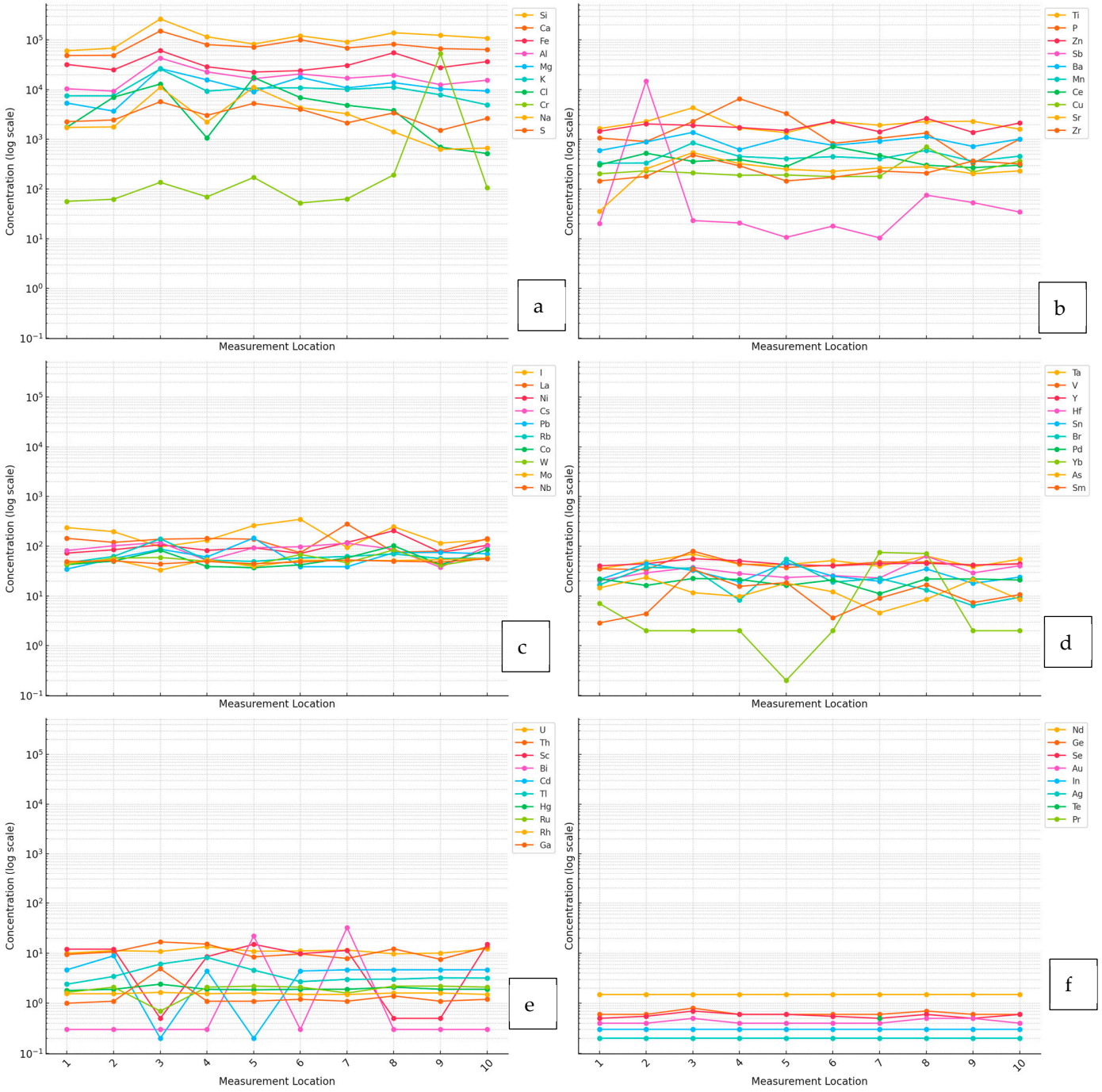

Figure 4. Logarithmic-scale representation of chemical element composition in particulate matter (PM) across sampling locations in Klaipėda, with elements grouped into six subfigures (**a**–**f**) by decreasing average concentration levels.

Each map in Figure 3 directly corresponds to its respective diagram in Figure 4, where Figure 3a aligns with Figure 4a, Figure 3b with Figure 4b, and so forth. The application of a logarithmic scale helps emphasize even minor concentration variations and enables more precise identification of significant element spikes, which may be associated with specific pollution sources.

In Figure 4, the chemical element concentrations at each measurement site are presented on a logarithmic scale, enhancing the visibility of differences between sampling locations. The horizontal axis represents the ten sampling sites, while the vertical axis indicates chemical element concentrations (mg/kg). Data points are connected by lines to ensure a clearer representation of concentration trends and facilitate the identification of significant fluctuations or anomalies that could indicate potential pollution sources.

The analysis of Figures 3 and 4 revealed that the highest concentrations of chemical elements in Klaipėda were associated with naturally occurring elements, particularly silicon (Si), aluminum (Al), calcium (Ca), and iron (Fe). Their relatively uniform distribution across different measurement locations suggests that these elements predominantly originate from natural sources, such as mineral dust, geological materials, construction activities, and road dust resuspension.

However, to distinguish whether certain elements are naturally occurring or linked to anthropogenic pollution, their distribution patterns, as revealed by the logarithmic scale, are crucial. Sharp fluctuations in the concentrations of specific elements at certain measurement sites may indicate localized pollution sources, most commonly associated with human activities. In contrast, when element concentrations remain relatively uniform across all measurement locations, this suggests that their sources are widespread in the environment and are likely of natural origin.

This is particularly evident at measurement station No. 3 (as shown in Figure 4), where exceptionally high concentrations of natural elements were detected, clearly influenced by bulk cargo handling at the port, which intensifies the emission and resuspension of mineral-rich particulate matter.

Unlike naturally occurring elements that exhibit a uniform spatial distribution, certain trace elements, such as chromium (Cr), antimony (Sb), ytterbium (Yb), and bismuth (Bi), demonstrated significant concentration fluctuations across measurement sites. Sharp increases in their concentrations at specific locations suggest potential localized pollution sources, most likely of anthropogenic origin.

This observed spatial variability underscores the importance of categorizing sampling points into clearly defined functional zones, enabling a more precise assessment of localized anthropogenic impacts linked to specific urban land-use patterns.

Accordingly, the sampling locations in Klaipėda were categorized into three functional zones based on their predominant characteristics and proximity to emission sources: port-industrial (No. 3, No. 4, No. 10), residential-urban (No. 5), and transport-dominated (No. 6, No. 7, No. 8, No. 9, No. 1, No. 2). For the port-industrial and transport-dominated zones, a zone-averaging approach was applied by calculating the arithmetic mean of the elemental concentrations from individual sampling locations. In contrast, the residential-urban zone, represented solely by a single sampling location (No. 5), relied on the recorded values without averaging. This introduces uncertainty, as the single sampling point may not adequately represent all residential areas in the city but rather only reflect conditions in the central residential area. This limitation should be taken into account when interpreting the results, as localized factors such as proximity to nearby roads or heating systems may influence the measurements at that single site. Other residential areas located further from major roads or away from the city center may exhibit different air quality characteristics due to lower traffic intensity or more open urban structures.

To enhance comparability between elements with significantly different concentration ranges, a logarithmic scale was employed in the visualization (Figure 5). This figure presents logarithmic concentration profiles for 59 chemical elements measured across three defined functional zones—port-industrial, residential-urban, and transport-dominated—in Klaipėda city. The horizontal axis lists the chemical elements, which are systematically ranked and grouped according to their relative dominance within each functional zone, while the vertical axis represents their concentrations (mg/kg) on a logarithmic scale.

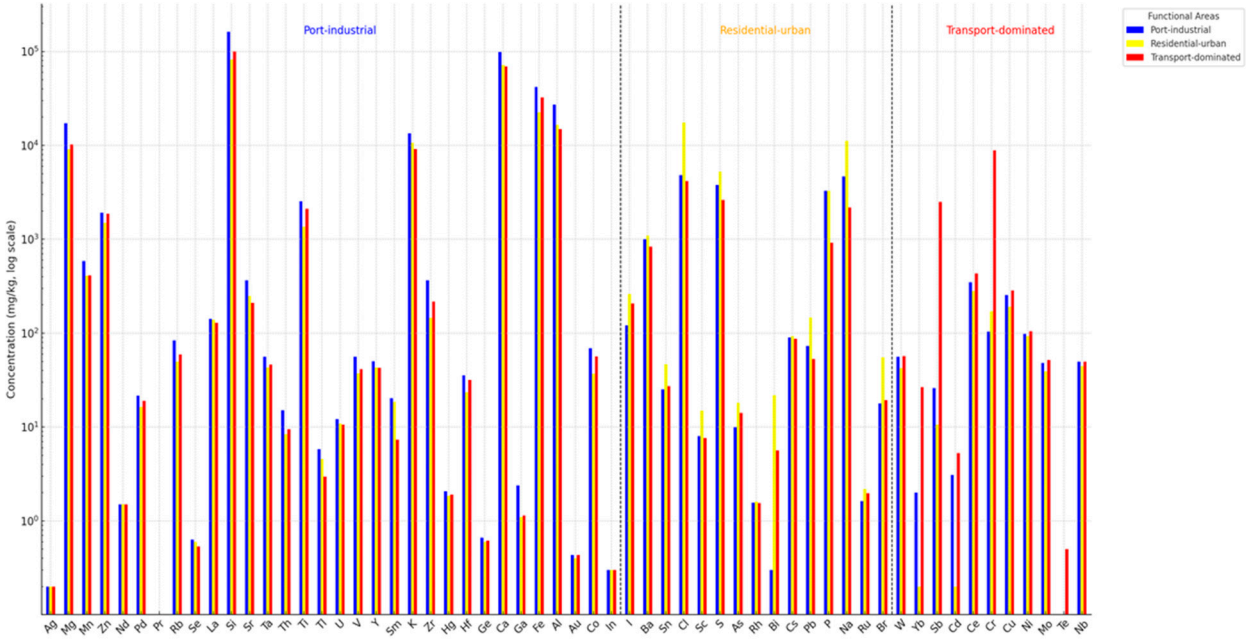

Figure 5. Chemical element composition of particulate matter (PM) across functional zones in Klaipėda: Port-Industrial, Residential, and Transport-Dominated areas.

Elements exhibiting the highest concentrations in the port-industrial zone are presented first, followed by those predominant in the residential-urban zone, and finally by those most prevalent in transport-dominated areas. Each functional zone is indicated using distinct colors, allowing clear visual differentiation of elemental concentration variations and spatial patterns. Such a structured visualization facilitates the identification of specific emission signatures and provides insights into the contributions of different pollutant sources characteristic of each urban functional area. This methodological approach effectively supports the detailed assessment of urban air quality.

After averaging the concentrations of chemical elements across different functional zones (Figures 1 and 5) and analyzing variations between specific measurement sites (Figure 4), distinct pollution patterns were observed:

- Port-industrial areas exhibit the highest concentrations of chemical elements. Despite the large number of detected elements and elevated total particulate matter (PM) concentrations, their composition remains predominantly natural, consisting mainly of mineral dust. Silicon (Si) and iron (Fe) are the dominant elements: Si concentrations reach 263,475 mg/kg (at station No. 3), 108,315 mg/kg (at No. 10), and 115,485 mg/kg (at No. 4), while Fe concentrations are recorded at 60,965 mg/kg (No. 3), 36,615 mg/kg (No. 10), and 27,715 mg/kg (No. 4). These findings align with Shen, J et al. (2019) [8] who reported that mineral particulate emissions in port areas primarily originate from bulk cargo handling operations, including iron ore, coal, and construction materials. Such emissions result from material loading, transportation, and wind erosion of stored bulk materials in open storage sites. Moreover, different port activities influence

pollution levels across measurement sites. Station No. 3, located at a dry bulk cargo terminal, exhibits particularly high Fe, Si, and Al concentrations, whereas Station No.4, which is dominated by a liquid bulk cargo terminal, has 2.28 times lower Si concentrations (115,485 mg/kg) compared to No. 3 (263,475 mg/kg). This significant difference can be explained by the fact that liquid bulk handling does not generate particulate emissions, resulting in significantly lower air pollution levels in this part of the port area.

Although Si, Fe, and Al are primarily natural elements, their exceptionally high concentrations at No. 3 (Figure 4) indicate a strong anthropogenic influence, where bulk cargo handling significantly enhances their presence in the atmosphere. This redistribution process leads to airborne concentrations that far exceed natural background levels, highlighting the role of port activities in shaping local air pollution dynamics.

- Transport-dominated zones exhibit elevated concentrations of anthropogenic metals, including Cr, Sb, Yb, Cu, Cd, and Ni, primarily linked to vehicle emissions. However, distinguishing whether these metals originate from anthropogenic or natural sources requires further examination of their distribution patterns. As seen in Figure 4, these metals exhibit significant concentration spikes at specific measurement sites, strongly suggesting localized transport-related emissions.

Chromium (Cr), a well-established marker of vehicular emissions, shows a sharp increase at station No. 9, a transport-dominated location, reinforcing its link to vehicle-related wear processes. Thorpe & Harrison (2008) [9] identified Cr as a key component of brake pad wear and road surface abrasion. Similarly, Wang et al. (2019) [7] demonstrated that Cr concentrations in urban environments are primarily associated with mechanical friction in vehicle braking systems. The elevated Cr concentrations in No. 9 suggest that frequent braking and road surface wear contribute significantly to localized Cr emissions in high-traffic areas.

Cadmium (Cd) exhibits notable spikes at stations No. 6, 7, 8, 9, and 10, of which No. 6–9 are transport-associated locations. Since these concentrations do not follow a uniform background distribution, but instead peak at sites with intense traffic, it can be inferred that Cd is primarily sourced from transport-related mechanical wear processes rather than natural geochemical inputs.

Copper (Cu) concentrations peak at station No. 2, another transport-heavy site, further confirming its strong association with braking activity. Boahen (2024) [10] identified Cu as a dominant metal in urban environments due to brake pad wear, where frictional material releases fine particles into the air and accumulates in road dust. Adachi and Tainosho (2004) [11] similarly found that Cu is among the most abundant elements in road dust samples from urban traffic zones, linking it directly to vehicle braking systems.

Ytterbium (Yb) concentrations increase significantly at stations No. 7 and No. 8, both of which are transport-associated sites. While Yb is not as well studied in vehicular emissions, previous research by Ji, X et al. (2023) [12] suggests that it may be released from mechanical wear of vehicle parts, particularly in diesel-powered engines. The localized enrichment of Yb at these sites suggests that its presence in PM is not a result of widespread natural geochemical sources, but instead stems from traffic-related emissions.

The distinct concentration spikes at these specific transport-related sites suggest that these metals do not originate from background natural sources but are instead linked to localized vehicle emissions. Unlike naturally occurring elements, which tend to exhibit a more uniform spatial distribution, the abrupt increases in Cr, Cd, Cu, and Yb concentrations at specific transport-heavy stations indicate anthropogenic contributions from vehicle-related processes such as brake wear, tire abrasion, road surface degradation, and fuel combustion.

These findings reinforce the critical role of vehicular emissions in urban air pollution and emphasize the need for improved emission control strategies. The presence of heavy metals such as Cu, Cr, and Ni—many of which are known to be toxic—suggests that long-term exposure in high-traffic areas could pose environmental and public health risks. Given the strong association between these metals and transport-related sources, regulatory interventions, such as stricter vehicle emission standards, alternative braking materials, and improved road maintenance, could significantly reduce metal contamination in urban environments [6]. Residential zones exhibit a complex chemical profile, integrating both natural and anthropogenic influences. Si (82,325 mg/kg) and Al (16,585 mg/kg) concentrations are lower than in port zones, as there is no direct contribution from bulk material handling. However, the most distinctive feature of this zone is the exceptionally high chlorine (Cl) concentrations (17,477.5 mg/kg), exceeding levels in both industrial and transport zones. Maasikmets et al. (2016) [13] identified domestic heating systems and waste combustion as significant sources of Cl emissions, particularly in areas where poor-quality fuel or waste materials are burned. The high Cl levels observed in this study align with their findings, indicating the influence of local combustion processes and transboundary pollution transport. Another notable element in residential zones is lead (Pb), which shows higher concentrations than in transport and industrial zones. The presence of Pb suggests a combination of legacy contamination from past emissions, as well as potential ongoing sources such as household heating, old lead-based paints, and contaminated soils. The association between Pb and domestic activities has been noted in previous studies, where low-quality fuels and waste burning have contributed to elevated Pb emissions. Furthermore, bismuth (Bi) concentrations (21.87 mg/kg) distinguish this zone, pointing to contributions from waste incineration and local heating systems.

These results reveal the distribution of air pollution across different functional zones of the city, highlighting distinct pollution sources and processes that determine the composition of particulate matter. Averaging the concentrations of chemical elements in these zones allows for the identification of dominant pollutants and, based on literature analysis, the estimation of their potential sources. While certain pollution trends—such as heavy metals associated with transportation or industrial dust emissions—are common to many cities, each urban environment has a unique combination of economic activities, infrastructure, and atmospheric conditions that shape its specific pollution profile. Klaipėda, as a port city, exhibits specific interactions between industrial, maritime, and transportation emissions, which may differ from trends observed in inland or highly urbanized cities. Therefore, while the spatial distribution of chemical elements provides a valuable basis for identifying pollution hotspots and potential sources, these data alone do not reveal whether different pollutants originate from separate or overlapping emission sources. To further investigate these relationships and refine pollution source attribution in Klaipėda, a correlation analysis was conducted.

3.2. Interrelationships Between Chemical Elements: Identifying Air Pollution Sources in Klaipėda

Building on the previous section, which categorized major chemical elements by their concentrations and linked them to potential pollution sources, correlation analysis provides a crucial next step in validating and refining these associations. Rather than focusing solely on individual pollutants, this approach evaluates whether elements are consistently emitted together, indicating common sources, or whether they co-occur due to secondary atmospheric processes.

To gain deeper insights into these interactions, a correlation analysis of chemical elements was conducted using Spearman's rank correlation coefficient. This method was chosen due to its ability to detect monotonic relationships between variables without as-

suming normal data distribution, making it particularly suitable for environmental studies where data often include outliers and values below detection limits. As described in the methodology section, the analysis was performed on a dataset comprising 59 chemical elements measured across 10 monitoring locations, allowing for a comprehensive evaluation of their interdependencies. Correlation analysis strengthens source attribution by determining whether specific elements consistently co-occur, implying a common pollution origin. Strong positive correlations ($r_s > 0.7$) suggest that elements are emitted simultaneously, either due to shared anthropogenic activities (e.g., industrial or vehicular emissions) or natural geochemical processes.

The correlation results are presented in Tables A2–A4, which were segmented for clarity due to the extensive size of the correlation matrix. Table 1 highlights strong positive correlations between various chemical elements, supporting the identification of dominant pollution sources and common geochemical interactions.

Table 1. Significant Positive Correlations Between Chemical Elements ($r_s > 0.7$).

Chemical Element	Chemical Element	Correlation	*p*-Value
Al	Ca	0.927	0.0002
W	Zn	0.915	0.0006
Hg	Rb	0.888	0.0008
Ta	W	0.879	0.002
Se	S	0.839	0.003
Sm	Se	0.826	0.003
Cr	Fe	0.818	0.003
Ca	Ga	0.753	0.01
Ga	Ba	0.753	0.01
Hf	Ga	0.753	0.01
Mg	K	0.745	0.01
Cd	Ga	0.733	0.01
Mn	Mg	0.733	0.01

The results of this study reveal that the distribution of chemical elements across different functional zones follows a distinct pattern and reflects specific emission trends. Correlation analysis demonstrated that, although certain chemical elements exhibit the highest concentrations in specific functional zones, as illustrated in Figure 5, they also display strong associations with elements dominant in other zones, suggesting a common emission source. Based on the analysis of chemical element distribution across functional zones and the assessment of their correlation patterns, three major pollution structures have been identified as key contributors to air quality in the city of Klaipėda.

3.2.1. Port-Transportation Interactions

The spatial distribution of zinc (Zn) and tungsten (W) concentrations highlights distinct emission trends: Zn concentrations are highest in the port, whereas W dominates in transport zones. However, a strong correlation between these elements ($r_s = 0.915$) suggests a shared emission source—transport activities. Zn and W are primarily associated with mechanical wear processes, with literature confirming that Zn emissions originate from tire wear and lubricant combustion, while W is released from brake systems and engine components [14] This correlation suggests that heavy-duty transport is a significant contributor to emissions, not only in transport zones but also in the port, where intensive vehicle movement facilitates Zn and W emissions.

Further reinforcing the link between transport and port activities is the strong correlation between chromium (Cr) and iron (Fe) ($r_s = 0.818$), indicating that these elements originate from both transport-related sources and industrial handling processes. Cr is

commonly associated with brake pad wear, road surface abrasion, and vehicle exhaust emissions, whereas Fe, in addition to natural geochemical sources, is emitted through industrial processes, cargo handling, and transport-related emissions [15]. Since increasing Cr concentrations indicate intensified traffic flow, while Fe emissions span both transport and industrial activities, their relationship serves as an indicator of overall economic and logistical activity: higher cargo handling volumes correlate with increased inbound and outbound transport, leading to rising Cr and Fe concentrations in the environment.

Although Fe can originate from natural geochemical processes, its concurrent increase with Cr in this context supports its classification as an anthropogenic pollutant linked to transport and industrial operations [15]. The observed correlations suggest that port and transport-related pollution are not independent but rather form an integrated pollution system. The Zn-W relationship highlights how the impact of heavy-duty transport extends beyond transport zones, significantly affecting port areas. Meanwhile, the Cr-Fe correlation not only reflects transport emissions but also serves as an indicator of economic intensification in the port, where Fe emissions are closely tied to cargo operations.

The strong correlation between cadmium (Cd) and gallium (Ga) (r_s = 0.733) complements the correlations observed between Fe-Cr and Zn-W, revealing a more comprehensive picture of the intertwined emissions from both transport and industrial activities. While Ga predominantly originates from industrial activities in the port, and Cd is a dominant pollutant in transport zones (Figure 5), the significant correlation between these two elements suggests a strong interconnection between transport and port emissions.

These findings underscore the need to assess air pollution as a complex, interlinked system where transport and industrial activities interact and reinforce one another, contributing to urban air quality deterioration. Recognizing these interdependencies can provide a foundation for more targeted and effective air quality management strategies, particularly in port cities where industrial and transport emissions overlap.

3.2.2. Port-Industrial Relationships

Mercury (Hg) and rubidium (Rb) emissions in port regions are primarily associated with industrial activities, including ship fuel combustion, metal refining, and cargo handling of metal-containing materials [16]. The results of this study confirm this association, as the highest concentrations of Hg and Rb were found in port zones (Figure 5), supporting their link to industrial emissions.

The strong correlation between Hg and Rb (r_s = 0.888) further suggests that high-temperature industrial processes—such as coal combustion, metal smelting, and waste incineration—serve as their primary emission sources. Hg is predominantly released from metal refining, fossil fuel combustion, and waste processing, whereas Rb originates from the volatilization of alkali metals in combustion residues [17].

In port regions, industrial operations significantly contribute to these emissions, particularly through ship fuel combustion, the handling of metal-rich cargo, and industrial manufacturing processes. The detection of these elements across all measurement sites suggests that pollution is not entirely localized, indicating that Hg and Rb can undergo atmospheric transport and deposition over both short and long distances [16]. Hg, in particular, is known to exist in both gaseous and particulate phases, facilitating long-range dispersion via dry and wet deposition mechanisms [18].

These findings reinforce the role of industrial port activities as a significant source of trace metal pollution, emphasizing the need for targeted monitoring and mitigation strategies in regions with high industrial density.

3.2.3. Resuspended Mineral Dust Contributions

The strong correlation between aluminum (Al) and calcium (Ca) concentrations (r_s = 0.927) and the moderate correlation between magnesium (Mg) and potassium (K) (r_s = 0.745) indicate that these elements follow common distribution patterns in the atmosphere. This relationship is explained by their natural co-occurrence in mineral dust particles, and their synchronized increase across measurement sites suggests that their resuspension is driven by common mechanical processes, such as transportation activity, cargo handling, and other port operations.

Although Al, Ca, Mg, and K are primarily associated with natural geochemical processes, their highest concentrations were recorded in the port area, particularly at measurement Site No. 3, highlighting the significant role of human activities in their mobilization into the atmosphere. Intensive mechanical disturbances, such as ship loading/unloading, heavy-duty vehicle movement, and cargo handling, contribute to dust resuspension, thereby increasing the concentration of these elements in the air. This process generates secondary emissions of suspended particles, significantly impacting overall particulate matter (PM) levels in urban air.

Moreover, it is essential to emphasize that mineral dust particles do not merely exist as passive natural components but can actively interact with other pollutants. Literature findings [15] suggest that such particles can adsorb heavy metals and transport-related emissions, forming secondary aerosol particles that remain in the atmosphere for extended periods and can be transported over considerable distances. This implies that, even though Al, Ca, Mg, and K originate from natural sources, their resuspension enhances environmental pollution by acting as carriers for other air pollutants.

Given that dust resuspension in the port is closely linked to human activities, targeted dust mitigation measures should be considered, including:

- Dust suppression technologies, such as water spraying or chemical dust binders in cargo handling areas.
- Optimization of heavy vehicle traffic flows to reduce mechanical disturbances and particle resuspension.
- Improvement of cargo handling procedures to minimize dust generation in industrial sites.

These findings demonstrate that resuspended mineral dust should not be viewed in isolation, as port activities clearly intensify its presence in the atmosphere and its interaction with other air pollutants. This highlights the need for an integrated air quality management strategy that not only addresses transport and industrial emissions but also actively incorporates dust control measures in ports and industrial zones.

3.3. Meteorological Influences on Air Pollution Dispersion and Accumulation in Klaipėda

The chemical composition of particulate matter (PM) reflects its diverse origins, including emissions from transportation, industrial activities, and natural sources. However, the distribution of these pollutants in urban environments is influenced not only by emission sources but also by meteorological conditions. In cities with high building density and intense traffic, air circulation can be restricted, leading to prolonged pollutant retention in certain areas [19].

Different pollutants exhibit distinct dispersion characteristics. Gaseous pollutants such as NO_2 disperse more easily due to their low molecular weight and ability to ascend into higher atmospheric layers, with the wind playing a crucial role in their dilution [20]. In contrast, PM is less affected by air movement, as heavier particles settle more easily on surfaces and can be resuspended by transportation and industrial activities [21].

To assess the impact of meteorological factors on air pollution concentrations, hourly air quality data from two state-operated real-time air pollution monitoring stations, marked as A and B in Figure 1, located in the city center and a high-traffic transportation zone, were analyzed. In addition to air pollution indicators (NO_2 and PM), meteorological parameters, including wind speed, atmospheric pressure, air temperature, and precipitation, were obtained from the Lithuanian Hydrometeorological Service (LHMT).

Given the complex interactions between air pollution and meteorological conditions, the Spearman correlation method (rs) was applied to evaluate monotonic relationships between meteorological variables and pollutant concentrations. This method was chosen for its suitability in environmental data analysis, particularly in cases where distributions may be non-normal or include outliers. The Spearman correlation coefficient helped determine whether statistically significant relationships exist between meteorological conditions and pollutant concentrations, specifically whether factors such as wind speed or precipitation significantly contribute to NO_2 or PM reduction in the city.

Figure 6 presents the relationship between NO_2 and PM concentrations and meteorological parameters. The vertical axis represents pollutant concentration ($\mu g/m^3$), while the horizontal axes depict four key meteorological variables: wind speed (m/s), air temperature (°C), atmospheric pressure (hPa), and precipitation (mm). PM concentrations are shown in red, while NO_2 concentrations are shown in blue.

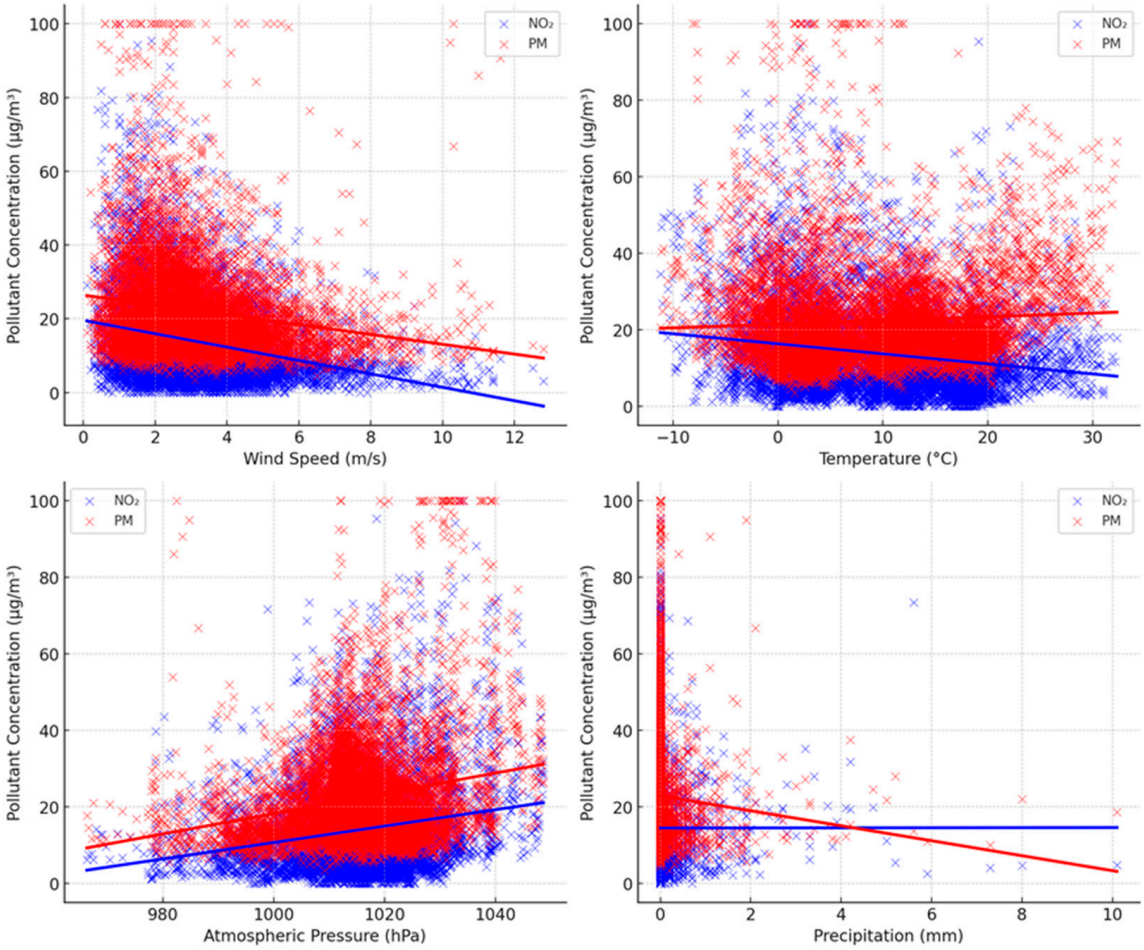

Figure 6. Spearman correlation between meteorological factors and air pollutants (Nitrogen Dioxide and Particulate Matter).

Figure 6 is based on hourly measurements from 2020 to 2023, providing a visual assessment of the relationship between meteorological conditions and pollutant concentrations. Each point in the diagrams represents an individual hourly measurement, allowing for an analysis of data density to identify conditions under which the highest pollutant concentrations occur. The trend lines in the graphs illustrate approximate tendencies between variables, offering insights into how pollutant levels change with varying meteorological parameters.

The results indicate that meteorological factors have a limited effect on reducing air pollution levels in the city. A moderate negative correlation between NO_2 and wind speed ($r_s = -0.270$) suggests that higher wind speeds contribute to NO_2 dilution. However, this effect is not strong enough to fully explain NO_2 variations in urban settings. Similar trends were observed by Vardaloukis [19] who noted that in urban street canyons, the impact of wind on NO_2 dispersion is reduced due to airflow disturbances caused by buildings.

A weak negative correlation between PM and wind speed ($r_s = -0.191$) indicates that PM dispersion is less sensitive to wind than NO_2. This can be explained by the fact that PM originates from diverse sources, including secondary resuspension processes driven by traffic and cargo handling activities. Zhang (2015) [20] found that PM movement in the atmosphere is influenced more by particle size and chemical composition than by direct wind impact.

Correlation analysis revealed that other meteorological factors do not exhibit strong relationships with pollutant concentrations. A weak negative correlation between NO_2 and temperature ($r_s = -0.183$) suggests that lower temperatures contribute to increased NO_2 levels not only due to changes in transportation emissions but also because of atmospheric chemical processes. At lower temperatures, the photochemical breakdown of NO_2 may decrease, while increased ozone (O_3) levels can facilitate additional conversion of NO to NO_2 [22].

A weak positive correlation between PM and temperature ($r_s = 0.110$) suggests that temperature does not significantly regulate PM concentrations. PM, as previous studies showed, is primarily influenced by local emission sources, such as transportation and industrial activities, rather than by temperature fluctuations.

A very weak correlation between atmospheric pressure and NO_2 ($r_s = 0.145$) and PM ($r_s = 0.144$) indicates that pressure fluctuations alone do not significantly affect air pollution levels. Similarly, a weak negative correlation between PM and precipitation ($r_s = -0.126$) suggests that rainfall has a limited role in removing PM from the atmosphere. Zhang et al. (2017) [23] found that precipitation significantly reduces PM concentrations only during intense rainfall events, which were not analyzed separately in this study.

These findings highlight that individual meteorological factors provide limited insight into urban air pollution patterns. Instead, a holistic approach is required, integrating meteorological data with urban structure characteristics, such as land use patterns, green spaces, and building density. In cities with high urbanization, air circulation is restricted, making it essential to examine not just meteorological conditions but also how built environments influence pollutant accumulation and dispersion.

4. Conclusions and Discussion

The results of this study demonstrate that air pollution in Klaipėda is driven by a complex combination of port activities, transport emissions, industrial operations, and household fuel combustion. Port areas, in particular, showed elevated levels of particulate matter (PM) and heavy metals, driven by bulk cargo handling, ship emissions, and related industrial processes. Strong correlations between key elements such as Cr–Fe, Zn–W,

and Cd–Ga indicate that multiple pollution sources are interacting and often spatially overlapping, especially in port and transport zones.

High chlorine concentrations in residential areas suggest the influence of domestic waste burning and fuel use, while traces of lead point to legacy pollution from older construction materials. These findings confirm that household sources also contribute significantly to urban air quality degradation and require further regulatory attention.

Meteorological analysis revealed that wind, temperature, and precipitation had a limited impact on pollutant dispersion, highlighting that emission intensity is the primary factor influencing pollution levels in the city. Therefore, relying on natural dispersion processes alone is insufficient, and active mitigation strategies must be prioritized.

Given Klaipėda's unique urban structure—where industrial, transport, and residential zones closely intersect—a comprehensive, interdisciplinary approach is essential for effective air quality management. Urban planning must integrate environmental considerations into zoning, infrastructure, and mobility strategies. Key measures include the development of ventilation corridors aligned with dominant wind directions, the installation of green buffer zones between industrial and residential areas, and optimized traffic management using synchronized traffic lights and pedestrian underpasses to reduce emissions from idling vehicles.

While rerouting port-related traffic may be limited due to the city's spatial constraints, targeted solutions such as time-restricted access zones, designated low-emission corridors, and the use of noise and dust barriers can reduce local impacts. These spatial strategies should be complemented by sector-specific actions, including the application of emission reduction technologies in port operations, stricter standards for vehicles, cleaner heating solutions in households, and the expansion of real-time air quality monitoring networks.

Collectively, these measures represent an adaptive, science-based framework for sustainable urban air quality management. Klaipėda, due to its urban-port integration, has the potential to serve as a model for similar coastal-industrial cities seeking to align economic development with environmental health.

Author Contributions: Conceptualization A.A.; Methodology A.A.; software A.A. and E.V.; investigation, A.A., E.V., S.S. and I.D.; writing and editing, A.A. and I.D.; visualization, A.A. and E.V.; supervision, I.D and S.S.; All authors have read and agreed to the published version of the manuscript.

Funding: This research received no external funding.

Institutional Review Board Statement: Not applicable.

Informed Consent Statement: Not applicable.

Data Availability Statement: The data presented in this study are available on request from the corresponding author.

Acknowledgments: The authors are grateful to UAB 'Klaipėdos paslaugos' for their cooperation in facilitating this research. Their support in permitting the installation of measurement devices on streetlight poles throughout Klaipeda city was invaluable to the study.

Conflicts of Interest: The authors declare no conflicts of interest.

Appendix A

Table A1. Methodological Framework.

Stage	Description
Sampling	Particulate matter (PM) samples were collected using passive samplers over four distinct seasonal campaigns (summer, autumn, winter, and spring) in 2023–2024. Each sampling period lasted approximately eight weeks to ensure the accumulation of sufficient PM mass for chemical analysis. Ten sampling sites were selected across Klaipėda to represent port-industrial, transport, and residential zones.
Sample preparation	The collected PM samples were dried at 45 °C for one hour and cooled in a desiccator to remove residual moisture. The dried material was homogenized using an agate mortar and pestle. For each sample, 0.050XX g of homogenized dust was mixed with 0.500XX g of wax to form a stable matrix for analysis. The mixture was gently blended to ensure uniformity and avoid altering the sample's structure before analysis. The notation "XX" indicates slight variation depending on weighing precision during preparation.
Chemical analysis	The chemical composition of PM was determined using X-ray fluorescence (XRF) spectroscopy with a SPECTRO XEPOS HE analyzer. This non-destructive technique enabled simultaneous detection and quantification of 59 chemical elements with high precision.
Data processing	Each site was analyzed four times to minimize random error, and the average values of elemental concentrations were calculated. Values below detection limits (BDL) were conservatively treated as equal to the detection threshold, following standard methodology.
Spatial and visual analysis	Dominant elements in each functional zone were identified and visualized using thematic maps and logarithmic-scale concentration diagrams. This allowed detection of element concentration spikes that may indicate anthropogenic influence.
Statistical analysis	Spearman correlation analysis was used to assess inter-element relationships and identify potential pollution sources. This method was chosen due to its robustness with non-normally distributed data. Correlation coefficients (rs) were interpreted based on strength (e.g., rs $\geq$ 0.70 indicating strong correlation), and statistical significance was assessed using *p*-values.
Meteorological correlation	Meteorological data (wind speed, direction, temperature, precipitation) from state monitoring stations were analyzed in parallel with PM concentrations to assess pollutant dispersion conditions and the role of weather in air quality variation.

Table A2. Spearman correlation matrix of chemical elements (Ag to Hr).

	Al	As	Au	Ba	Bi	Br	Ca	Cd	Ce	Cl	Co	Cr	Cs	Cu	Fe	Ga	Ge	Hf
Al	1.000	−0.515	0.266	0.370	0.009	−0.030	0.927	−0.736	0.212	0.212	0.006	0.103	0.188	−0.370	0.285	0.629	0.548	0.176
As	−0.515	1.000	0.038	−0.309	−0.234	0.248	−0.297	0.078	−0.115	0.309	−0.515	−0.006	−0.285	0.067	−0.588	−0.396	−0.137	−0.164
Au	0.266	0.038	1.000	0.418	−0.325	−0.266	0.418	−0.082	−0.494	−0.038	0.418	0.722	−0.114	0.494	0.494	0.529	0.661	0.570
Ba	0.370	−0.309	0.418	1.000	0.242	0.455	0.503	−0.293	−0.200	0.479	0.527	0.479	0.612	0.370	0.370	0.753	0.548	0.564
Bi	0.009	−0.234	−0.325	0.242	1.000	0.493	−0.009	−0.181	−0.035	0.398	−0.208	0.052	0.294	−0.450	−0.303	−0.278	−0.188	−0.528
Br	−0.030	0.248	−0.266	0.455	0.493	1.000	0.103	−0.228	0.321	0.927	−0.091	−0.261	0.673	−0.212	−0.273	0.026	0.274	−0.236
Ca	0.927	−0.297	0.418	0.503	−0.009	0.103	1.000	−0.723	0.139	0.394	−0.006	0.212	0.200	−0.273	0.139	0.733	0.548	0.273
Cd	−0.736	0.078	−0.082	−0.293	−0.181	−0.228	−0.723	1.000	0.078	−0.430	0.436	−0.156	−0.052	0.488	0.085	−0.317	−0.505	0.150
Ce	0.212	−0.115	−0.494	−0.200	−0.035	0.321	0.139	0.078	1.000	0.285	−0.042	−0.842	0.503	−0.503	−0.152	0.032	0.000	−0.212
Cl	0.212	0.309	−0.038	0.479	0.398	0.927	0.394	−0.430	0.285	1.000	−0.200	−0.127	0.539	−0.285	−0.297	0.162	0.411	−0.176
Co	0.006	−0.515	0.418	0.527	−0.208	−0.091	−0.006	0.436	−0.042	−0.200	1.000	0.176	0.455	0.661	0.818	0.551	0.411	0.636
Cr	0.103	−0.006	0.722	0.479	0.052	−0.261	0.212	−0.156	−0.842	−0.127	0.176	1.000	−0.273	0.527	0.224	0.298	0.274	0.503
Cs	0.188	−0.285	−0.114	0.612	0.294	0.673	0.200	−0.052	0.503	0.539	0.455	−0.273	1.000	−0.042	0.236	0.441	0.548	0.152
Cu	−0.370	0.067	0.494	0.370	−0.450	−0.212	−0.273	0.488	−0.503	−0.285	0.661	0.527	−0.042	1.000	0.479	0.305	0.137	0.782
Fe	0.285	−0.588	0.494	0.370	−0.303	−0.273	0.139	0.085	−0.152	−0.297	0.818	0.224	0.236	0.479	1.000	0.474	0.548	0.479
Ga	0.629	−0.396	0.529	0.753	−0.278	0.026	0.733	−0.317	0.032	0.162	0.551	0.298	0.441	0.305	0.474	1.000	0.603	0.753
Ge	0.548	−0.137	0.661	0.548	−0.188	0.274	0.548	−0.505	0.000	0.411	0.411	0.274	0.548	0.137	0.548	0.603	1.000	0.411
Hf	0.176	−0.164	0.570	0.564	−0.528	−0.236	0.273	0.150	−0.212	−0.176	0.636	0.503	0.152	0.782	0.479	0.753	0.411	1.000

Table A3. Spearman correlation matrix of chemical elements (Hg to Rb).

	Hg	I	Y	Yb	K	La	Mg	Mn	Mo	Na	Nb	Ni	P	Pb	Pd	Rb
Hg	1.000	−0.355	0.683	−0.029	0.526	−0.328	0.683	0.744	−0.027	−0.027	−0.007	0.560	0.027	0.348	0.393	0.888
I	−0.355	1.000	−0.491	−0.426	0.103	−0.564	−0.200	−0.067	−0.115	0.139	−0.224	−0.358	−0.018	−0.018	−0.105	−0.321
Y	0.683	−0.491	1.000	−0.050	0.285	0.200	0.345	0.576	−0.030	0.139	0.127	0.673	0.576	0.333	0.198	0.564
Yb	−0.029	−0.426	−0.050	1.000	−0.188	0.634	0.020	−0.366	−0.020	−0.327	0.475	0.079	−0.139	−0.822	−0.010	0.198
K	0.526	0.103	0.285	−0.188	1.000	−0.333	0.745	0.576	−0.685	0.588	−0.612	0.321	0.382	0.370	0.303	0.503
La	−0.328	−0.564	0.200	0.634	−0.333	1.000	−0.188	−0.188	−0.006	0.079	0.333	0.176	0.406	−0.370	−0.173	−0.248
Mg	0.683	−0.200	0.345	0.020	0.745	−0.188	1.000	0.733	−0.164	0.321	−0.370	0.152	0.212	0.188	0.395	0.503
Mn	0.744	−0.067	0.576	−0.366	0.576	−0.188	0.733	1.000	−0.091	0.188	−0.127	0.539	0.418	0.515	0.346	0.539
Mo	−0.027	−0.115	−0.030	−0.020	−0.685	−0.006	−0.164	−0.091	1.000	−0.552	0.661	−0.224	−0.394	−0.261	−0.303	−0.152
Na	−0.027	0.139	0.139	−0.327	0.588	0.079	0.321	0.188	−0.552	1.000	−0.552	0.055	0.479	0.139	−0.284	0.115
Nb	−0.007	−0.224	0.127	0.475	−0.612	0.333	−0.370	−0.127	0.661	−0.552	1.000	0.333	−0.224	−0.467	−0.445	0.115
Ni	0.560	−0.358	0.673	0.079	0.321	0.176	0.152	0.539	−0.224	0.055	0.333	1.000	0.370	0.345	−0.074	0.648
P	0.027	−0.018	0.576	−0.139	0.382	0.406	0.212	0.418	−0.394	0.479	−0.224	0.370	1.000	0.297	0.142	−0.103
Pb	0.348	−0.018	0.333	−0.822	0.370	−0.370	0.188	0.515	−0.261	0.139	−0.467	0.345	0.297	1.000	0.284	0.127
Pd	0.393	−0.105	0.198	−0.010	0.303	−0.173	0.395	0.346	−0.303	−0.284	−0.445	−0.074	0.142	0.284	1.000	0.093
Rb	0.888	−0.321	0.564	0.198	0.503	−0.248	0.503	0.539	−0.152	0.115	0.115	0.648	−0.103	0.127	0.093	1.000

Table A4. Spearman correlation matrix of chemical elements (Rh to Zr).

	Rh	**Ru**	**S**	**Sb**	**Sc**	**Se**	**Si**	**Sm**	**Sn**	**Sr**	**Ta**	**Th**	**Ti**	**Tl**	**U**	**V**	**W**	**Zn**	**Zr**
Rh	1.000	0.257	0.359	0.334	−0.494	0.416	0.434	0.585	0.283	0.321	0.170	0.132	0.434	0.522	−0.644	0.208	−0.107	−0.120	0.227
Ru	0.257	1.000	0.000	0.329	−0.019	0.033	0.108	0.108	0.184	−0.247	−0.070	−0.298	−0.133	0.120	−0.286	−0.234	−0.152	0.139	−0.197
S	0.359	0.000	1.000	−0.127	−0.062	0.839	0.382	0.624	0.648	0.479	0.697	0.588	−0.030	0.382	−0.043	0.261	0.539	0.576	−0.079
Sb	0.334	0.329	−0.127	1.000	−0.309	0.184	0.273	0.018	0.139	0.103	0.382	0.345	0.527	0.236	−0.249	0.018	0.297	0.382	0.359
Sc	−0.494	−0.019	−0.062	−0.309	1.000	−0.100	−0.827	−0.222	0.315	−0.389	−0.259	−0.173	−0.784	−0.161	0.430	−0.556	−0.278	−0.031	−0.545
Se	0.416	0.033	0.839	0.184	−0.100	1.000	0.464	0.826	0.489	0.674	0.801	0.807	−0.006	0.642	0.121	0.477	0.521	0.559	0.296
Si	0.434	0.108	0.382	0.273	−0.827	0.464	1.000	0.503	−0.115	0.442	0.612	0.370	0.612	0.261	−0.280	0.758	0.491	0.309	0.675
Sm	0.585	0.108	0.624	0.018	−0.222	0.826	0.503	1.000	0.333	0.745	0.539	0.455	0.030	0.685	0.000	0.648	0.188	0.152	0.407
Sn	0.283	0.184	0.648	0.139	0.315	0.489	−0.115	0.333	1.000	0.224	0.491	0.224	−0.055	0.139	−0.195	−0.164	0.382	0.552	−0.444
Sr	0.321	−0.247	0.479	0.103	−0.389	0.674	0.442	0.745	0.224	1.000	0.600	0.636	0.297	0.624	0.243	0.636	0.442	0.273	0.419
Ta	0.170	−0.070	0.697	0.382	−0.259	0.801	0.612	0.539	0.491	0.600	1.000	0.782	0.321	0.285	0.049	0.564	0.879	0.830	0.365
Th	0.132	−0.298	0.588	0.345	−0.173	0.807	0.370	0.455	0.224	0.636	0.782	1.000	0.127	0.455	0.267	0.418	0.685	0.636	0.365
Ti	0.434	−0.133	−0.030	0.527	−0.784	−0.006	0.612	0.030	−0.055	0.297	0.321	0.127	1.000	0.164	−0.371	0.297	0.285	0.067	0.529
Tl	0.522	0.120	0.382	0.236	−0.161	0.642	0.261	0.685	0.139	0.624	0.285	0.455	0.164	1.000	0.304	0.164	−0.103	−0.055	0.450
U	−0.644	−0.286	−0.043	−0.249	0.430	0.121	−0.280	0.000	−0.195	0.243	0.049	0.267	−0.371	0.304	1.000	−0.036	0.006	0.030	0.149
V	0.208	−0.234	0.261	0.018	−0.556	0.477	0.758	0.648	−0.164	0.636	0.564	0.418	0.297	0.164	−0.036	1.000	0.455	0.188	0.693
W	−0.107	−0.152	0.539	0.297	−0.278	0.521	0.491	0.188	0.382	0.442	0.879	0.685	0.285	−0.103	0.006	0.455	1.000	0.915	0.122
Zn	−0.120	0.139	0.576	0.382	−0.031	0.559	0.309	0.152	0.552	0.273	0.830	0.636	0.067	−0.055	0.030	0.188	0.915	1.000	−0.085
Zr	0.227	−0.197	−0.079	0.359	−0.545	0.296	0.675	0.407	−0.444	0.419	0.365	0.365	0.529	0.450	0.149	0.693	0.122	−0.085	1.000

References

1. Murphy, S.M.; Agrawal, H.; Sorooshian, A.; Padró, L.T.; Gates, H.; Hersey, S.; Welch, W.A.; Jung, H.; Miller, J.W.; Cocker, D.R.; et al. Comprehensive Simultaneous Shipboard and Airborne Characterization of Exhaust from a Modern Container Ship at Sea. *Environ. Sci. Technol.* **2009**, *43*, 4626–4640. [CrossRef] [PubMed]
2. Pandolfi, M.; Gonzalez-Castanedo, Y.; Alastuey, A.; de la Rosa, J.D.; Mantilla, E.; de la Campa, A.S.; Querol, X.; Pey, J.; Amato, F. Source apportionment of PM_{10} and $PM_{2.5}$ at multiple sites in the Strait of Gibraltar by PMF: Impact of shipping emissions. *Environ. Sci. Pollut. Res.* **2011**, *18*, 260–269. [CrossRef] [PubMed]
3. Ramsey, N.R.; Klein, P.M.; Moore, B., III. The impact of meteorological parameters on urban air quality. *Atmos. Environ.* **2014**, *86*, 58–67. [CrossRef]
4. Andriulė, A.; Vasiliauskienė, E.; Rapalis, P.; Dailidienė, I. Air Pollution in the Port City of Lithuania: Characteristics of the Distribution of Nitrogen Dioxide and Solid Particles When Assessing the Demographic Distribution of the Population (2023). *Sustainability* **2024**, *16*, 8413. [CrossRef]
5. Smith, R.B.; Beevers, S.D.; Gulliver, J.; Dajnak, D.; Fecht, D.; Blangiardo, M.; Douglass, M.; Hansell, A.L.; Anderson, H.R.; Kelly, F.J.; et al. Impacts of air pollution and noise on risk of preterm birth and stillbirth in London. *Environ. Int.* **2020**, *134*, 105290. [CrossRef]
6. Grigoratos, T.; Martini, G. Brake wear particle emissions: A review. *Environ. Sci. Pollut. Res.* **2014**, *22*, 2491–2504. [CrossRef]
7. Wang, Y.; Wang, L.; Petäjä, T.; Zha, Q.; Gong, C.; Li, S.; Pan, Y.; Hu, B.; Xin, J.; Kulmala, M. Increased inorganic aerosol fraction contributes to air pollution and haze in China. *Atmos. Chem. Phys.* **2019**, *19*, 5881–5888. [CrossRef]
8. Shen, J.; Feng, X.; Zhuang, K.; Lin, T.; Zhang, Y.; Wang, P. Vertical distribution of particulates within the near-surface layer of dry bulk port and influence mechanism: A case study in China. *Sustainability* **2019**, *11*, 7135. [CrossRef]
9. Thorpe, A.; Harrison, R.M. Sources and properties of non-exhaust particulate matter from road traffic: A review. *Sci. Total Environ.* **2008**, *400*, 270–282. [CrossRef]
10. Boahen, E. Heavy metal contamination in urban roadside vegetables: Origins, exposure pathways, and health implications. In *Discover Environment*; Springer: Berlin/Heidelberg, Germany, 2024.
11. Adachi, K.; Tainosho, Y. Characterization of heavy metal particles embedded in tire dust. *Environ. Int.* **2004**, *30*, 1009–1017. [CrossRef]
12. Ji, X.; Xiong, J.; Guan, W.; Qi, Y.; Zhou, L.; Li, H. Effects of hot extrusion on the microstructure and wear properties of A380-Yb alloy. *Metals* **2023**, *14*, 1343. [CrossRef]
13. Maasikmets, M.; Kupri, H.-L.; Teinemaa, E.; Vainumäe, K.; Arumäe, T.; Roots, O.; Kimmel, V. Emissions from burning municipal solid waste and wood in domestic heaters. *Atmos. Pollut. Res.* **2016**, *7*, 438–446. [CrossRef]
14. Skorbiłowicz, M.; Sidoruk, M. Assessment of heavy metal content and identification of their sources in bottom sediments and various macrophyte species of the Narew River (Poland). *Minerals* **2025**, *15*, 8. [CrossRef]
15. Birmili, W.; Allen, A.G.; Bary, F.; Harrison, R.M. Trace Metal Concentrations and Water Solubility in Size-Fractionated Atmospheric Particles and Influence of Road Traffic. *Environ. Sci. Technol.* **2006**, *40*, 1144–1153. [CrossRef] [PubMed]
16. Moldanová, J.; Fridell, E.; Popovicheva, O.; Demirdjian, B.; Tishkova, V.; Faccinetto, A.; Focsa, C. Characterisation of particulate matter and gaseous emissions from a large ship diesel engine. *Atmos. Environ.* **2009**, *43*, 2632–2641. [CrossRef]
17. Streets, D.G.; Devane, M.K.; Lu, Z.; Bond, T.C.; Sunderland, E.M.; Jacob, D.J. All-time releases of mercury to the atmosphere from human activities. *Environ. Sci. Technol.* **2011**, *45*, 10485–10491. [CrossRef]
18. Rea, A.W.; Lindberg, S.E.; Keeler, G.J. Dry deposition and foliar leaching of mercury and selected trace elements in deciduous forest throughfall. *Atmos. Environ.* **2001**, *35*, 3453–3462. [CrossRef]
19. Vardoulakis, S.; Fisher, B.E.; Pericleous, K.; Gonzalez-Flesca, N. Modelling air quality in street canyons: A review. *Atmos. Environ.* **2003**, *37*, 155–182. [CrossRef]
20. Zhang, X.; Davidson, E.A.; Mauzerall, D.L.; Searchinger, T.D.; Dumas, P.; Shen, Y. Managing nitrogen for sustainable development. *Nature* **2015**, *528*, 51–59. [CrossRef]
21. Amato, F.; Pandolfi, M.; Escrig, A.; Querol, X.; Alastuey, A.; Pey, J.; Perez, N.; Hopke, P.K. Quantifying road dust resuspension in urban environment by Multilinear Engine: A comparison with PMF. *Atmos. Environ.* **2009**, *43*, 2770–2780. [CrossRef]
22. Zar, J.H. Spearman Rank Correlation. In *Biostatistical Analysis*, 5th ed.; Pearson Prentice-Hall: Hoboken, NJ, USA, 2005; pp. 378–386.
23. Zhang, B.; Jiao, L.; Xu, G.; Zhao, S.; Tang, X.; Zhou, Y.; Gong, C. Influences of wind and precipitation on different-sized particulate matter concentrations ($PM_{2.5}$, PM_{10}, $PM_{2.5–10}$). *Meteorol. Atmos. Phys.* **2017**, *129*, 291–304. [CrossRef]